ISSN 1674-1056
http://cpb.iphy.ac.cn
http://iopscience.iop.org/cpb
中国物理 B
Chinese Physics
中国物理
Chinese Physics B

Light slowing and all-optical time division multiplexing of hybrid four-wave mixing signal in nitrogen-vacancy center

Ruimin Wang(王瑞敏), Irfan Ahmed, Faizan Raza, Changbiao Li(李昌彪), Yanpeng Zhang(张彦鹏)
Citation: Chin. Phys. B . 2020, 29(5): 054204 . **doi:** 10.1088/1674-1056/ab7b50
Journal homepage: http://cpb.iphy.ac.cn; http://iopscience.iop.org/cpb

What follows is a list of articles you may be interested in

Numerical investigation on coherent mid-infrared supercontinuum generation in chalcogenide PCFs with near-zero flattened all-normal dispersion profiles

Jie Han(韩杰), Sheng-Dong Chang(常圣东), Yan-Jia Lyu(吕彦佳), Yong Liu(刘永)
Chin. Phys. B . 2019, 28(10): 104204 . **doi:** 10.1088/1674-1056/ab3f25

Enhancement and control of the Goos-Hänchen shift bynonlinear surface plasmon resonance in graphene

Qi You(游琪), Leyong Jiang(蒋乐勇), Xiaoyu Dai(戴小玉), Yuanjiang Xiang(项元江)
Chin. Phys. B . 2018, 27(9): 094211 . **doi:** 10.1088/1674-1056/27/9/094211

Research progress of third-order optical nonlinearity of chalcogenide glasses

Xiao-Yu Zhang(张潇予), Fei-Fei Chen(陈飞飞), Xiang-Hua Zhang(章向华), Wei Ji(季伟)
Chin. Phys. B . 2018, 27(8): 084208 . **doi:** 10.1088/1674-1056/27/8/084208

Nonlinear spectral cleaning effect in cross-polarized wave generation

Linpeng Yu(於林鹏), Yi Xu(许毅), Fenxiang Wu(吴分翔), Xiaojun Yang(杨晓骏), Zongxin Zhang(张宗昕), Yuanfeng Wu(吴圆峰), Yuxin Leng(冷雨欣), Zhizhan Xu(徐至展)
Chin. Phys. B . 2018, 27(5): 054214 . **doi:** 10.1088/1674-1056/27/5/054214

Modulation and mechanism of ultrafast transient spectroscopy based on dimethylamino-carbaldehyde derivatives

Tong-xing Jin(金桐兴), Jun-yi Yang(杨俊义), Yu Fang(方宇), Yan-bing Han(韩艳兵), Ying-lin Song(宋瑛林)
Chin. Phys. B . 2018, 27(5): 054208 . **doi:** 10.1088/1674-1056/27/5/054208

Light slowing and all-optical time division multiplexing of hybrid four-wave mixing signal in nitrogen-vacancy center*

Ruimin Wang(王瑞敏)[1,†], Irfan Ahmed[2,3], Faizan Raza[1], Changbiao Li(李昌彪)[1], and Yanpeng Zhang(张彦鹏)[1,2,‡]

[1] School of Science & Key Laboratory for Physical Electronics and Devices of the Ministry of Education & Shaanxi Key Laboratory of Information Photonic Technique, Xi'an Jiaotong University, Xi'an 710049, China
[2] Department of Physics, City University of Hong Kong, Kowloon, Hong Kong SAR, China
[3] Electrical Engineering Department, Sukkur IBA University, 65200, Sindh, Pakistan

(Received 16 November 2019; revised manuscript received 15 January 2020; accepted manuscript online 1 March 2020)

We report the experimental results of hybrid four-wave mixing and fluorescence signals from nitrogen-vacancy (NV) centers in diamond. The fluorescence signals are slowed owing to dark state. The observed delay time of light slowing due to interconversion between NV^- and NV^0 is about 6.4 μs. The relative intensities of read-out signals change with the wavelength and power of writing pulse. Based on light slowing, we present the model of all-optical time division multiplexing. The intensity ratio in different demultiplexed channels is modulated by the wavelength and power of control field. It has potential applications in quantum communication and all-optical network.

Keywords: nonlinear optics, fluorescence, time division multiplexing

PACS: 42.65.–K, 42.79.Sz **DOI:** 10.1088/1674-1056/ab7b50

1. Introduction

Many applications in quantum communication and quantum computation require long coherence time in room temperature. Recently, quantum coherence effects in nitrogen-vacancy center (NV center) have drawn much attention because of its prominent spin properties of solid in room temperature. The electron spin of NV^- center has a long coherence time up to 1.8 ms.[1,2] The decay of excited triplet states ^3E through metastable singlet states via intersystem crossing (ISC)[3,4] could prepare population onto $m_s = 0$ state and thus lead to spin polarization.[5] A long-living dark state was observed,[6] which has been suggested to be the neutral NV^0.[7] It was shown that optical excitation can induce interconversions between NV^- and NV^0.[8,9] These advances on NV center research have enabled numerous applications including optical switching,[8] quantum register,[10] quantum sensor,[11,13] routing and single-photon device.[14] In quantum information and all-optical network, it is necessary to have devices such as quantum repeater and all-optical routing, where optical information can be transferred and distributed among different channels.[15]

Former studies on light emissions from NV center focus on the linear spectra. Nonlinear spectra of NV center, especially spectra in time domain has been reported very seldom till now. In this paper, we perform time domain measurements of spontaneous four-wave mixing (SFWM) and multi-order fluorescence (FL) obtained from NV centers. It is shown that fluorescence can be slowed owing to dark state. We also observed damped Rabi oscillations of SFWM signals. We modified the intensity rate of signal in different channels by varying the power and frequency of incident laser pulses. Based on light slowing due to interconversion between two charge states NV^- and NV^0, we present the model of all-optical time division multiplexing. The approach of optical data storage by conversion of charge states has been reported in rare-earth ion recently.[16] This approach has high conversion efficiency and low read-out power. Moreover, it has the potential to be extented to two-dimensional (2D) and three-dimensional (3D) memory.

2. Experiment

The sample used in our experiment is a ⟨100⟩ oriented single crystal diamond and contains less than 5-ppb nitrogen concentration. Figure 1(a) presents the energy levels of NV^- and NV^0. The NV^- center has two triplet states, named ground state $^3A_2$ and excited state ^3E, and two singlet states ($^1A_1$, ^1E). The transition between ^3E and $^3A_2$ has a resonant wavelength of 638 nm. The nonradiative transition of populations in ^3E ($m_s = \pm 1$) via ISC to singlet states can prepare population onto $^3A_2$ ($m_s = 0$) and thus lead to spin polarization. The main transition of NV^0 has resonant wavelength of 575 nm. The interconversions between NV^- and NV^0 can be induced by ionization and recombination. Two tunable dye lasers with 0.04-cm^{-1} linewidth pumped by an

*Project supported by the National Key Research and Development Program of China (Grant Nos. 2017YFA0303700 and 2018YFA0307500) and the National Natural Science Foundation of China (Grant Nos. 61605154, 11604256, and 11804267).

†Corresponding author. E-mail: wangrm@mail.xjtu.edu.cn
‡Corresponding author. E-mail: ypzhang@mail.xjtu.edu.cn

© 2020 Chinese Physical Society and IOP Publishing Ltd

injection locked single mode Nd:YAG laser (Continuum Powerlite DLS 9010, 10-Hz repetition rate, 5-ns pulse width) are used to generate the control field E_1 (637 nm) and probe field E_2 (575 nm). We can construct two-level and V-type three-level systems from these fine-structure levels.

Figure 1(b) shows our experimental scheme. In V-type three-level system with two fields E_1 and E_2 illuminating sample, two SFWM signals (Stokes E_S and anti-Stokes E_{AS} beams) are reflected by polarized beam splitter (PBS) and collected by two photomultiplier tubes (PMT) D1 and D2. The SFWM process satisfies the phase-matching condition $\boldsymbol{k}_S = \boldsymbol{k}_1 + \boldsymbol{k}_2 - \boldsymbol{k}_{AS}$ and $\boldsymbol{k}_{AS} = \boldsymbol{k}_1 + \boldsymbol{k}_2 - \boldsymbol{k}_S$, respectively. Where $\boldsymbol{k}_{1,2}$ is the wavevector of the pumping field and $\boldsymbol{k}_{S/AS}$ is the wavevector of generated Stokes E_S and anti-Stokes E_{AS} beams. In a two-level system with one control field E_1 switched on, the phase-matching condition is $\boldsymbol{k}_S = 2\boldsymbol{k}_1 - \boldsymbol{k}_{AS}$ and $\boldsymbol{k}_{AS} = 2\boldsymbol{k}_1 - \boldsymbol{k}_S$, respectively. The FL signal is generated accompanying the SFWM process. Another PMT (D3) placed at near position is used to collect the FL signal. A fast gated integrator is used to control measuring range in time domain. All data are detected at room temperature.

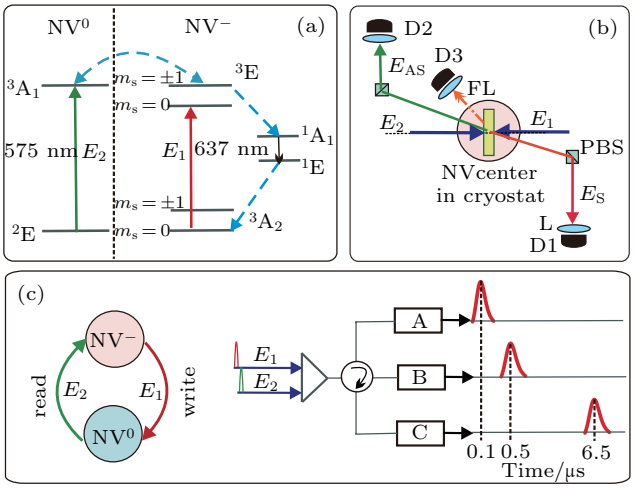


Fig. 1. (a) Energy level diagram of NV centers. (b) Schematic diagram of the experimental arrangement. D1, D2, D3: photomultiplier tubes, PBS: polarized beam splitter, L: lens. (c) The model of all-optical time division multiplexing.

3. Results and discussion

In our experiment, the FL signal is generated accompanying the SFWM process. Figure 2 demonstrates the obtained hybrid signal in the two-level system. First, we set the measuring range of gated integrator at 20 μs from pumping field is on (0 μs). One can see two peaks in time domain. A sharp peak is followed by a broad peak labeled as peak C. The further measurements for left peak is conducted when the range of gated integrator is set from 0 μs to 2 μs. It reveals two fine structures named peaks A and B as shown in the inset of Fig. 2(a). There are about 0.4-μs and 6-μs delay times between peaks A, B, and C, respectively. We attribute the fast emission signal of peak A to SFWM signal, while two delayed signals peaks B and C to the second-order fluorescence processes. In peak A, the signal shows typical exponential decay. We fit peak with a single exponential decay function and obtain the decoherence time $\tau_a = 0.2$ μs. On the other hand, as shown in Fig. 2(b), the peak B cannot be fitted by single exponential decay function. The fitting parameter of peak B changes from $\tau_1 = 0.6$ μs to $\tau_2 = 0.3$ μs, which indicates multiple relaxation channels. The peak C is fitted with a single exponential decay function and obtain decoherence time $\tau_c = 6$ μs which is much longer than peaks A and B.

We consider the optical transition between spin-triplet ground states $^3A_2$ and excited states ^3E with resonant excitation. In the two-level system $|0\rangle\,(^3A_2,\ m_s = 0) \rightarrow |1\rangle\,(^3E,\ m_s = 0)$ with one control field E_1 switched on, the second-order fluorescence signal is generated through the perturbation chain $\rho_{00}^{(0)} \xrightarrow{\omega_1} \rho_{10}^{(1)} \xrightarrow{\omega_1} \rho_{11}^{(2)}$, the diagonal density matrix element is given by

$$\rho_{11}^{(2)} = G_1^2/(\Gamma_{10} + \mathrm{i}\Delta_1)\Gamma_{11}, \tag{1}$$

where Δ_1 is the detuning of the pumping field, ρ_{ij} is the diagonal density matrix element, and Γ_{ij} is the decoherence rate between levels $|i\rangle$ and $|j\rangle$. The decoherence rate of FL is given as $\Gamma_{FL} = 1/\tau = \Gamma_{10} + \Gamma_{11}$.

For SFWM process the perturbation chains can be described as $\rho_{00}^{(0)} \xrightarrow{\omega_1} \rho_{10}^{(1)} \xrightarrow{\omega_{as}} \rho_{00}^{(2)} \xrightarrow{\omega_1} \rho_{10(s)}^{(3)}$ (Stokes) and $\rho_{00}^{(0)} \xrightarrow{\omega_1} \rho_{10}^{(1)} \xrightarrow{\omega_s} \rho_{00}^{(2)} \xrightarrow{\omega_1} \rho_{10(as)}^{(3)}$ (anti-Stokes) via the Liouville pathway method and respective the density matrix elements can be written as

$$\rho_s^{(3)} = -\mathrm{i}G_{as}^* G_1^2/(\Gamma_{10} + \mathrm{i}\Delta_1)^2[\Gamma_{00} + \mathrm{i}(\Delta_1 - \Delta_{as})], \tag{2}$$

$$\rho_{as}^{(3)} = -\mathrm{i}G_s^* G_1^2/(\Gamma_{10} + \mathrm{i}\Delta_1)^2[\Gamma_{00} + \mathrm{i}(\Delta_1 - \Delta_s)]. \tag{3}$$

We can obtain the decoherence rate of SFWM signal as $\Gamma_{FWM} = 1/\tau_a = 2\Gamma_{10} + \Gamma_{00}$. The hybrid signals including three stages can be described as

$$\begin{aligned} I(t) \ = \ & \rho_{S/AS}^{(3)}\, \mathrm{e}^{-G_i^2 t^2} \otimes \mathrm{e}^{-\Gamma_a t} + \rho_b^{(2)}\, \mathrm{e}^{-[(t-t_b)^2]/w^2} \otimes \mathrm{e}^{-\Gamma_b t} \\ & + \rho_c^{(2)}\, \mathrm{e}^{-[(t-t_c)^2]/w^2} \otimes \mathrm{e}^{-\Gamma_c t}, \end{aligned} \tag{4}$$

where the subscript letters a, b, and c denote three peaks in Fig. 2. $G_i = -\mu E_i/\hbar$ is the Rabi frequency of the pumping fields, w is the pulse width, $t_{b,c}$ is the delayed time of peaks B and C, $\Gamma_{a,b,c}$ is the decoherence rate. Based on the cross-Kerr nonlinear interaction between photons of different states, the hybrid correlation is realized by the coupling between SFWM and second-order FL signals, which can be used as a new type of qubit.[17] Moreover, there are different delay times between SFWM and two FL signals, we can obtain three-channel time division multiplexing.

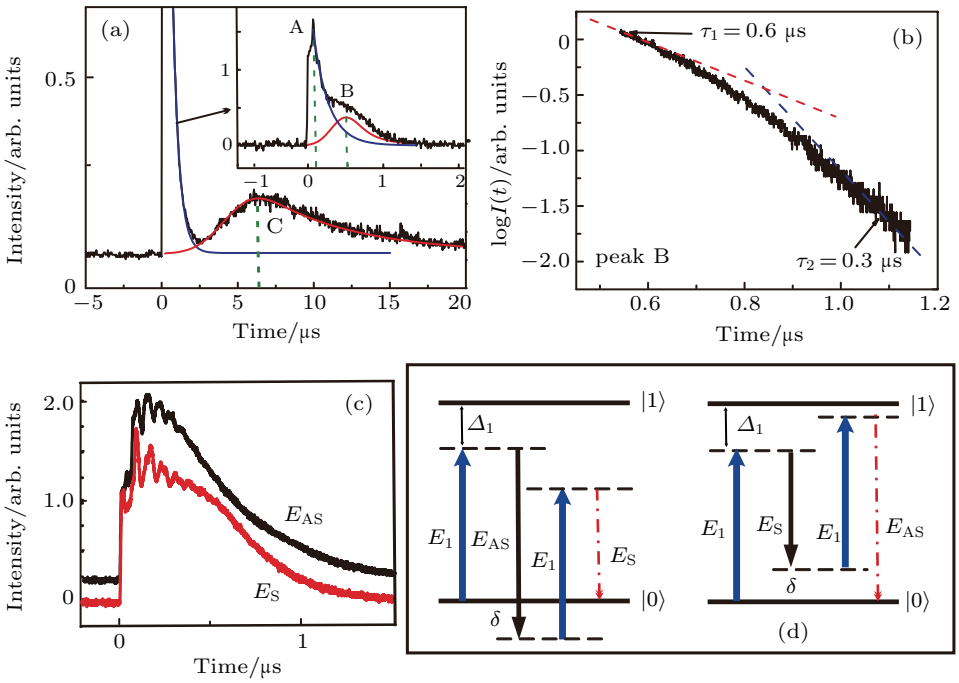


Fig. 2. (a) Hybrid signal under the illumination of 637-nm pulse laser in time domain. The red and blue lines in both figures are fitting curves. The graph at the top right corner (inset) is the zoom-in of the left peak at gated integrator range set from 0 μs to 2 μs. (b) The value $\log I(t)$ measured at peak B. (c) The Rabi oscillations of peak A for Stokes and anti-Stokes beams. (d) Two FWM generation channels in the two-level system.

First, we focus on the SFWM signals of peak A. Figure 2(c) presents Stokes and anti-Stokes signals collected by D1 and D2. Both Stokes and anti-Stokes signals exhibit damped Rabi oscillation in time-domain. In the two-level system, the SFWM signals can be generated through two channels[18] as shown in Fig. 2(d). The nonlinear susceptibilities of Stokes signal can be written as

$$\chi_S^{(3)}(\delta) = \frac{N\mu_{10}}{\varepsilon_0 E_1 E_1 E_{as}^*}\rho_S^{(3)}(\delta) = \frac{-iN\mu_{10}^4}{\varepsilon_0\hbar^3}\frac{1}{(\Gamma_{10}+i\Delta_1)(\Gamma_{00}-i\delta)[\Gamma_{10}+i(\Delta_1-\delta)][\Gamma_{10}+i(\delta+\Delta_1)]}, \tag{5}$$

where N is the atomic density and μ_{ij} is the dipole matrix element between levels $|i\rangle$ and $|j\rangle$. From Eq. (5) one can see, Stokes signal has three resonances at $\delta = 0$ and $\delta = \pm\Delta_1$. This is the so-called triplet-resonance structure in frequency domain. The Rabi oscillation of SFWM signal is produced by the interferences of two frequencies at ω_1 and $\omega_1 \pm \Delta_1$. Distinguishing the oscillation of two-photon correlation with delay time $\tau = t_S - t_{AS}$,[19,20] we call such oscillation of FWM signal with time t_S as self-correlation oscillation. The time-domain signal intensity is given by the Fourier transform

$$\langle E_s^- E_s^+\rangle = R_s\left(\int d\delta\, e^{-i\omega_s t_s}\chi_s^{(3)}\Phi\left(\frac{2\delta L}{v_s}\right)\right)^2. \tag{6}$$

In our experiment the nonlinear effect is dominant, the longitudinal detuning function can be defined as $\Phi(2\delta L/v_s) = 1$, so we can obtain

$$\begin{aligned}\langle E_s^- E_s^+\rangle &= R_s\left(\int d\delta\chi_s^{(3)} e^{-i\omega_s t_s}\right)^2 \\ &= 4R_s\left(\frac{-iN\mu_{10}^4}{\varepsilon_0\hbar^3}\right)^2[e^{-2\Gamma_{00}t_s} + e^{-2\Gamma_{10}t_s} \\ &\quad - 2\cos(\Delta_1 t_s)e^{-(\Gamma_{00}+\Gamma_{10})t_s}],\end{aligned} \tag{7}$$

where $R_s = (E_1^2 L\omega_S)^2/[2c(\Gamma_{10}+i\Delta_1)]^2$. Therefore, the SFWM signal exhibits Rabi oscillation.

Next, we discuss delayed FL signals. For peak B, FL signals are from transitions between ^{3}E manifold to ^{3}A$_2$ manifold. There are two possible transition pathways $|m_s = 0\rangle \to |m_s = 0\rangle$ and $|m_s = \pm1\rangle \to |m_s = \pm1\rangle$ for spin-conserving optical transitions. Considering the interaction of electron with phonon in the diamond lattice, a spin-dependent nonradiative transition into a metastable state, the so-called intersystem crossing (ISC), will modulate the FL lifetimes of two transition pathways. The spin states of ^{3}E show different ISC rate into the spin-singlet state ^{1}A$_1$.[3,4] Electrons in $m_s = \pm1$ have significant chance to decay to spin-singlet state, while the ISC rate of $m_s = 0$ has been established to be negligible when compared with $m_s = \pm1$ states. Thus, the decoherence rate of $m_s = \pm1$ should add an additional nonradiative item Γ_{ISC}. At room temperature, considering the spin mixing processes, the averaged ISC rate for all ^{3}E states with $m_s = \pm1$ can be written as follows:[3,4]

$$\Gamma_{ISC} = \frac{1}{4}(\Gamma_{A_1} + 2\Gamma_{E_{1,2}}), \tag{8}$$

$$\Gamma_{A_1} = 4\pi\hbar\lambda_\perp^2 \sum_n |\langle\chi_0 \mid \chi_n\rangle|^2 \delta(\nu_n - \Delta) = 4\pi\hbar\lambda_\perp^2 F(\Delta), \quad (9)$$

$$\Gamma_{E_{1,2}} = 2\pi\hbar^3 \sum_{n,p,k} \left|\frac{\sqrt{2}\lambda_\perp \lambda_{p,k}}{\omega}\right|^2 \left|\left\langle \chi_0 \left| \chi_n' \right\rangle\right|^2 \times [(n_{p,k}+1)\delta(\nu_n + \omega_k - \Delta) + n_{p,k}\delta(\nu_n - \omega_k - \Delta)], \quad (10)$$

where Γ_{A_1} and $\Gamma_{E_{1,2}}$ are the ISC rates of fine level A_1 and $E_{1,2}$ of ^{3}E states with $m_s = \pm 1$, $F(\Delta) = \sum_n |\langle\chi_0|\chi_n\rangle|^2 \delta(\nu_n - \Delta)$ is the vibrational overlap function. Therefore, spin-dependent intersystem crossing induces double exponential decay in peak B. Furthermore, we can prepare population onto $^3A_2$ ($m_s = 0$) and thus leading to spin polarization.

Figure 3(a) shows the comparison of intensity ratio between SFWM signal peak A and FL signal peak B under different pumping fields. In the two-level system with one pumping field, one can see the FL intensity of peak B under 637-nm resonant excitation is stronger than 575-nm non-resonant excitation. Figure 3(a3) shows the FL signal excited by control field E_1 (637 nm) and probe field E_2 (575 nm) in the three-level system. The FL intensity of peak B excited by two laser pulses is obviously stronger than 575-nm non-resonant excitation. The delay times of FL peak B in three cases are all about 0.4 μs, which do not change with the control field.

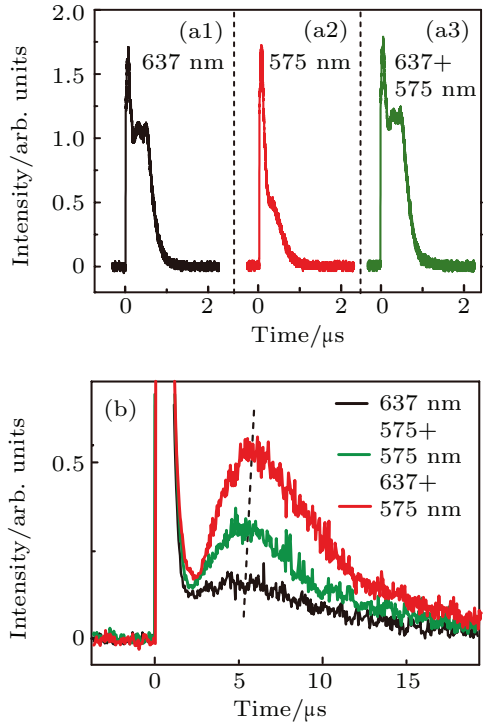


Fig. 3. (a) Peaks A and B pumped under different laser wavelengths. (b) Peak C pumped under different laser wavelengths.

At peak C, there is a long rise time before the signal reaches maxima, which origins from the accumulation of excited population. After that the signal shows typical exponential decay. A long-living dark state was reported in NV center,[6] and it has now been suggested to be NV^0.[7] We attribute the significantly delayed peak C to ionization and recombination processes between NV^- and NV^0. Photoionization from NV^- to NV^0 can occur through two-photon absorption followed by an Auger process when the excitation wavelength is longer than 575 nm.[8,9] One photon excites an electron from the energy level $^3A_2$ to ^{3}E of NV^-. If the second photon is captured before the radiative recombination from excited state ^{3}E, the excited electron can be detached from defect to the conduction band of the diamond, and leading NV^- converting to NV^0. On the other hand, the recombination process from NV^0 back to NV^- can also be induced by two-photon absorption. One photon excites an electron to the excited state of NV^0, the second photon excites an electron from valence band into the gap and be acquired by NV^0, which converts NV^0 back to NV^-. Such a conversion between NV^- to dark state NV^0 induces obvious slowing of FL peak C. Figure 3(b) shows the frequency-dependence of peak C. We first compare the intensities of peak C excited by one pumping field (637 nm) in the two-level system with which by control and probe fields (637 nm+575 nm) in the three-level system. One can see that the intensity of peak C excited by two laser pulses is much greater than that with one excitation field. It is because that the recombination rate from NV^0 to NV^- becomes small when the photon energy is much less than the zero phonon line of NV^0(wavelength is longer than 600 nm).[20,21] The long-living dark state NV^0 can be used for optical storage. As shown in Fig. 1(c), two laser beams 637 nm and 575 nm are used as writing and reading pulses, respectively. In writing process, NV^- converts to NV^0 induced by 637-nm resonant excitation. The fluorescence read-out is done at 575-nm excitation, and lead NV^0 back to NV^-. The resonant excitation of NV^0 can effectively convert it into negatively charge state at very low power. Because ionization and recombination processes can occur circularly, so this optical storage is rewritable. We also compare the writing efficiency of 637-nm and 575-nm laser pulses. When the writing pulse change from 637 nm to 575 nm, the intensity of read-out FL signal (575 nm+575 nm) decreases. It indicates that the ionization efficiency from NV^- to NV^0 under 637-nm resonant excitation is greater than 575-nm non-resonant excitations. Next, we compare the delay time of peak C in three cases. One can see the delay time (6.4 μs) excited by 637-nm+575-nm pulses is longer than that under 575-nm+575-nm pulses (5.6 μs) and 637-nm single pulse excitation (5.2 μs). We can conclude that the optimum intensity and light slowing effect of read-out signal can be obtained when 637-nm and 575-nm laser beams are used as writing and reading pulses, respectively.

Based on the relative time delay of hybrid signals, we

present a model of all-optical time division multiplexing or routing. As shown in Fig. 1(c), there are three demultiplexed channels, one FWM and two FL signal channels. Excited by control field E_1 and probe field E_2, the read-out signals can have 0.4 μs and 6.4 μs delay time between channels A–B and A–C, respectively. In order to characterize the de-multiplexing effect, we express the contrast index as $\eta = (t_i - t_j)/(t_i + t_j)$, $i, j = \mathrm{A}, \mathrm{B}, \mathrm{C}$. Where $t_i - t_j$ is time gap between abutting channels. In our experiment, the contrast index reaches 67% and 85% for channels A–B and B–C, respectively. The high contrast index indicates the peaks will become more separated. So the time division multiplexing can avoid crosstalk effectively in all-optical communication.

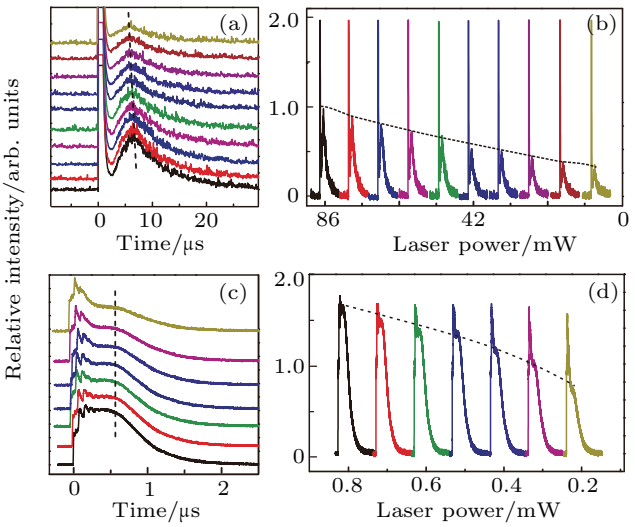


Fig. 4. The intensity ratios of signals in three demultiplexed channels change with the power of control field. (a) and (b) Relative delay time and intensity ratio between peak A and peak C. The read-out power keeps 8 mW. (c) and (d) Relative delay time and intensity ratio between peak A and peak B. The read-out power is 0.2 mW.

In order to modulate signals among three demultiplexed channels, we observe the relative intensity ratio of read-out signals in three channels by changing laser power of control field E_1, while the read-out power of E_2 keeps 8 mW. Figures 4(a) and 4(b) show relative delay time and intensity ratio between peaks A and C at different control powers. With control power increasing from 0.8 mW to 8 mW, the relative intensity ratio of peak C/A changes from about 1/10 to 1/2. For two-photon process, both ionization and recombination rates are proportional to the excitation power $k_{\mathrm{ion/re}} \propto I^2$.[17] At larger powers, the populations transferred from NV^- to NV^0 increase. As a consequence, the intensity ratio of peak C/A increases. The delay time only increase 0.5 μs when the power changes from 0.8 mW to 8 mW. Figures 4(c) and 4(d) show the corresponding results of peaks A and B. With control power increasing from 0.2 mW to 0.8 mW, the intensity ratio of peak B/A increases from 1/2 to 1/1. However, we do not observe changes in delay time between peaks A and B. It is mean that the time gap between demultiplexed channels can remain stable when the signal intensity is modulated. According to our results, we can modulate the signals of different demultiplexed channels by the power of control field. Such dynamic modulation can meet communication demands of each channel at different time, and then to improve plant availability. It also has potential applications in quantum computation.

4. Conclusion

In summary, we measured the hybrid signal including SFWM and second-order FL from NV centers. Two FL peaks show different delay times to SFWM signal. It is attributed to ionization–recombination process between two charge states and spin polarization from metastable state, respectively. The time delay of light slowing due to interconversion between NV^- and NV^0 is about 6.4 μs. The delay time excited by 637-nm single pulse is shorter than that excited by 637-nm +575-nm writing and reading pulses. The intensity of read-out signal is determined by the wavelength of writing pulse. The larger intensity of read-out signal can be obtained when 637-nm and 575-nm laser beams are used as writing and reading pulses, respectively. We also investigated delayed signals at different powers of writing pulse. The relative intensity ratio between SFWM and read-out FL signal shows obvious dependence on the power of writing pulse. The relative intensity ratio of peak C/A increases significantly with the power of writing pulse. The delay time increases slightly with power. Based on two delayed read-out signals, we present a model of all-optical time division multiplexing. The intensity ratio of different channels has been modulated by frequency and power of control field. This controllable system combining the behaviors of optical storage and all-optical time division multiplexing has potential applications in all-optical communication and quantum computation.

References

[1] Maurer P C, Kucsko G, Latta C, Jiang L, Yao N Y, Bennett S D, Pastawski F, Hunger D, Chisholm N, Markham M, Twitchen D J, Ciac J I and Lukin M D 2012 *Science* **336** 1283
[2] Balasubramanian G, Neumann P, Twitchen D, Markham M, Kolesov R, Mizuoschi N, Isoya J, Achard J, Beck J, Tissler J, Jacques V, Hemmer P R, Jelezko F and Wrachtrup J 2009 *Nat. Mater.* **8** 383
[3] Goldman M L, Sipahigil A, Doherty M W, Yao N Y, Bennett S D, Markham M, Twitchen D J, Manson N B, Kubanek A and Lukin M D 2015 *Phys. Rev. Lett.* **114** 145502
[4] Goldman M L, Doherty M W, Sipahigil A, Yao N Y, Bennett S D, Manson N B, Kubanek A and Lukin M D 2015 *Phys. Rev. B* **91** 165201
[5] Manson N B, Harrison J P and Sellars M J 2006 *Phys. Rev. B* **74** 104303
[6] Han K Y, K I M S K, Eggeling C and Hell S W 2010 *Nano Lett.* **10** 3199
[7] Waldherr G, Beck J, Steiner M, Neumann P, Gali A, Frauenheim Th, Jelezko F and Wrachtrup J 2011 *Phys. Rev. Lett.* **106** 157601
[8] Siyushev P, Pinto H, Voros M, Gali A, Jelezko F and Wrachtrup J 2013 *Phys. Rev. Lett.* **110** 167402
[9] Chen X D, Zou C L, Sun F W and Guo G C 2013 *Appl. Phys. Lett.* **103** 013112

[10] Dutt M V G, Childress L, Jiang E T L, Maze J, Jelezko F, Zibrov A S, Hemmer P R and Lukin M D 2007 *Science* **316** 1312
[11] Maze J R, Stanwix P L, Hodges J S, Hong S, Taylor J M, Cappellaro P, Jiang L, Dutt M V G, Togan E, Zibrov A S, Yacoby A, Walsworth R L and Lukin M D 2008 *Nature* **455** 644
[12] Shang Y X, Hong F, Dai J H, Yu H, Lu Y N, Liu E K, Yu X H, Liu G Q and Pan X Y 2019 *Chin. Phys. Lett.* **36** 086201
[13] Ye J F, Jiao Z, Ma K, Huang Z Y, Lv H J and Jiang F J 2019 *Chin. Phys. B* **28** 047601
[14] Li S, Li C H, Zhao B W, Dong Y, Li C C, Chen X D, Ge Y S and Sun F W 2017 *Chin. Phys. Lett.* **34** 096101
[15] Wang H H, Fan Y F, Wang R, Wang L, Du D M, Kang Z H, Jiang Y, Wu J H and Gao J Y 2009 *Opt. Lett.* **34** 2596
[16] Riesen N, Pan X Z, Badek K, Ruan Y L, Monro T M, Zhao J B, Heidepriem H E and Riesen H 2018 *Opt. Express* **26** 12266
[17] Wang R M, Pargorn P, Raza F, Ahme I, Wang H X and Zhang Y P 2018 *Laser Phys. Lett.* **15** 085401
[18] Du S W, Wen J M, Rubin M H and Yin G Y 2007 *Phys. Rev. Lett.* **98** 053601
[19] Du S W, Oh Eun, Wen J M and Rubin M H 2007 *Phys. Rev. B* **76** 013803
[20] Aslam N, Waldherr G, Neumann P, Jelezko F and Wrachtrup J 2013 *New J. Phys.* **15** 013064
[21] Han K Y, Wildanger D, Rittweger E, Meijer J, Pezzagna S, Hell S W and Eggeling C 2012 *New J. Phys.* **14** 123002